

See discussions, stats, and author profiles for this publication at: <https://www.researchgate.net/publication/227340956>

Connection between the Upper and Lower Energy Regions of the Potential Energy Surface of the Ground Electronic State of the HSO₂ System

ARTICLE in THE JOURNAL OF PHYSICAL CHEMISTRY A · JUNE 2012

Impact Factor: 2.69 · DOI: 10.1021/jp302755f · Source: PubMed

CITATIONS

2

READS

22

4 AUTHORS:



Gabriel Freitas

Petróleo Brasileiro S.A.

3 PUBLICATIONS 8 CITATIONS

[SEE PROFILE](#)



Juan D Garrido

Universidade Federal da Integração Latino-A...

13 PUBLICATIONS 87 CITATIONS

[SEE PROFILE](#)



Maikel Y Ballester

Federal University of Juiz de Fora

17 PUBLICATIONS 72 CITATIONS

[SEE PROFILE](#)



Marco Nascimento

Federal University of Rio de Janeiro

143 PUBLICATIONS 1,912 CITATIONS

[SEE PROFILE](#)

Connection between the Upper and Lower Energy Regions of the Potential Energy Surface of the Ground Electronic State of the HSO_2 System

Gabriel N. Freitas,[†] Juan D. Garrido,[‡] Maikel Y. Ballester,[§] and Marco Antonio Chaer Nascimento*,[†]

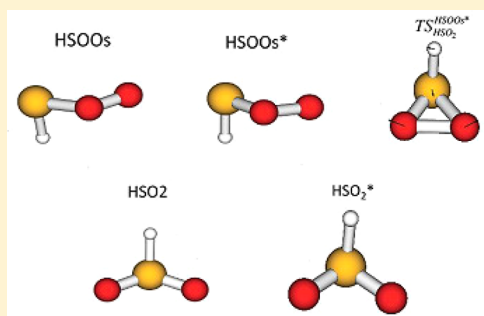
[†]Departamento de Físico-Química, Instituto de Química, Universidade Federal do Rio de Janeiro, Rio de Janeiro, 21941-590 RJ, Brazil

[‡]Universidade Federal da Integração Latino-Americana, Foz do Iguaçu, 85867-970 PR, Brazil

[§]Departamento de Física, ICE, Universidade Federal de Juiz de Fora, 36036-330 MG, Brazil

Supporting Information

ABSTRACT: The importance of the HSO_2 system in atmospheric and combustion chemistry has motivated several works dedicated to the study of associated structures and chemical reactions. Nevertheless, controversy still exists about a possible connection between the upper and lower energy regions of the potential energy surface (PES) for the ground electronic state of the system. Very recently, a path to connect these regions was proposed based on studies at the CASPT2/aug-cc-pV(T+d)Z level of calculation but the small energy difference between some of the transitions states along that path suggested the necessity of calculations at a higher level of theory. In the present work, we report a CCSD(T)/aug-cc-pV(T+d)Z study of the stationary states associated to the proposed connection path, including assessment of the most reliable complete basis set (CBS) extrapolation scheme for the system. Among the new features, the present calculations show that there are no structures corresponding to the $\text{HSO}_2(\text{b})$ minimum and the TS3 saddle point obtained at the CASPT2 level and that the connection path between the upper and lower energy regions of the PES for the ground electronic state involves only one transition state and most probably more than one electronic state.



1. INTRODUCTION

The importance of sulfur as a major contaminant in different environmental issues such as acid rain, air pollution, and global climate changes has been well established.^{1–3} In addition, sulfur compounds have significant impact on fuel combustion processes.^{4–7} In particular, isomers of HSO_2 have been recognized as important structures for understanding the atmospheric and combustion chemistry.

The potential energy surface (PES) for the electronic ground-state (EGS) of HSO_2 has been studied in several works.^{8–34} According to these studies, the mentioned PES could be divided in two energy regions: the first one, hereafter denoted as lower-energy region, includes the global minimum and the asymptotic limits^{12,13,16,22,27} $\text{OH} + \text{SO}$ and $\text{H} + \text{SO}_2$. The second one, which will be referred to as the upper-energy region, comprises the HSOO isomers, together with the $\text{HSO} + \text{O}$ and $\text{HS} + \text{O}_2$ dissociation limits.^{19,25,27,32,34} The connection between these two energy regions has not been well determined up to now. While Marshall and co-workers,¹⁹ based on second order Møller–Plesset perturbation theory calculations (MP2), have shown that all attempts to connect the HSOO and HSO_2 isomers led to the dissociation $\text{HSO} + \text{O}$, Ballester and Varandas have located a transition state (TS) connecting the $\text{HSO}\cdots\text{O}$ van der Waals minimum with the HSO_2 radical in their global double many-body expansion

potential energy surface (DMBE).²⁷ However Sendt and co-workers³² have discarded such possibility because they could not find this transition state in calculations at the complete active space self-consistent field (CASSCF) level of theory.

A recent work by Garrido et al.,³⁴ using the Rayleigh–Schrödinger second-order perturbation theory (CASPT2), corroborated the above-mentioned finding of Sendt and co-workers. However, they found another path connecting the two energy regions of the PES containing two transition states and one local minimum. Nevertheless, the small energy difference between the stationary states along the proposed path suggests a reinvestigation at a higher level of theory.

The major goal of the present work is, therefore, to report higher level ab initio calculations for the stationary states connecting the lower and upper energy regions of the electronic ground state of the HSO_2 system in order to clarify the topology of the PES along such a connection and to better characterize the chemical structure of all species involved in the connecting path. Additionally, we will investigate the possibility of electronic state crossing along the aforementioned connection.

Received: March 22, 2012

Revised: June 15, 2012

Published: June 18, 2012



The article is organized as follows: section 2 provides a brief description of the ab initio calculations, and the results are presented and discussed in section 3, whereas the major conclusions are gathered in section 4.

2. COMPUTATIONAL METHODS

The open-shell coupled cluster theory with single and double excitations and perturbative triples correction (CCSD(T))^{35–39} was used to calculate the geometries, total energies, harmonic vibrational frequencies, zero point vibrational energies, and CBS limits of the stationary points linking the lower and upper energy regions of the PES for the EGS of the HSO₂ system. In the calculations, high-spin restricted-open Hartree–Fock wave functions (ROHF) are used as reference, and this approach will be referred to as ROCCSD(T). Considering that the standard correlation-consistent polarized valence hierarchy (cc-pVXZ) basis sets^{40,41} present some difficulties for dealing with sulfur containing systems,^{42–45} we have used the Dunning's correlation consistent basis^{46,47} containing extra tight d functions denoted by aug-cc-pV(X+d)Z for the S atom and aug-cc-pVXZ for the H and O atoms. Geometry optimizations were carried out for X = T. For the sake of simplicity, from here on, we shall use the notation aV(X+d)Z for these basis sets. Unless explicitly specified, all the optimized geometries, total energies, complete basis set extrapolation (CBS), zero-point vibration energies (ZPE), and frequencies reported throughout the article are obtained at the same level of the theory.

Transition states were confirmed by inspection of the vibration frequencies, while connections with reactants and products were determined by intrinsic reaction coordinate (IRC) calculations.⁴⁸ As starting guesses for the geometry optimizations, we have used the corresponding structures previously obtained.³⁴ All ab initio calculations were carried out with the MOLPRO program.⁴⁹ Exceptionally, state-averaged complete active-space self-consistent field (SA-CASSCF)⁵⁰ were performed with the Columbus program⁵¹ in order to determine minimum energy points in the electronic states crossing seam.

Following the methodology implemented in MOLPRO,⁴⁹ the rational functional approach⁵² has been used as the search algorithm for the minima, while the quadratic steepest descend method has been employed to locate the transition states configurations. Such a method was also used to determine the reaction path (intrinsic reaction coordinate). The harmonic vibrational frequencies and ZPE for all stationary points were computed at the same level of theory using numerical Hessians as implemented in MOLPRO⁴⁹ without the consideration of any scaling factor.⁵³

Single-point calculations using aV(X+d)Z basis sets with X = 3–5 were carried out for the CBS extrapolations, and two different approaches were employed for evaluating the CBS extrapolated energies. The first one considers separately the extrapolation of the reference and the correlation energies, while the second deals directly with the total electronic energies. The different approaches and levels of extrapolation used are distinguished by a label followed by the number of points considered in the extrapolation. The number 2 will be used to indicate that the energies obtained with basis sets X = 4,5 were used in the fitting and the number 3 when the energies obtained with X = 3,4,5 were used.

Within the first approach, two formulas were tested for the ROHF energy extrapolation. The first one was the three-parameter proposed by Feller:⁵⁴

$$E_X^{\text{HF}} = E_{\infty}^{\text{HF}} + B \exp(-CX) \quad (1)$$

which will be denoted as HF-3. The other one is a more recently proposed 2-parameter formula,^{55,56} referred to as HF-2:

$$E_X^{\text{HF}} = E_{\infty}^{\text{HF}} + B(X + 1) \exp(-9\sqrt{X}) \quad (2)$$

As for the extrapolation of the correlation energies, we used the well-known 2-parameter equation proposed by Helgaker:⁵⁷

$$E_X^{\text{cor}} = E_{\infty}^{\text{cor}} + BX^{-3} \quad (3)$$

and the uniform singlet-pair and triplet-pair extrapolation (USTE) proposed by Varandas:⁵⁸

$$E_X^{\text{cor}} = E_{\infty}^{\text{cor}} + \frac{A_3}{(X + \alpha)^3} + \frac{A_5^0 + cA_3^m}{(X + \alpha)^5} \quad (4)$$

with the recommended values of the parameters $\alpha = -3/8$, $A_5^0 = 1.1660699(E_h)$, and $c = -1.4222512$ for $m = 1$, for coupled-cluster calculations.⁵⁸ The results obtained with these last two expressions are designated as CLAS-*n* and USTE-*n*, respectively.

For the second approach, we used the 3-parameter equation PET-3:

$$E_X^{\text{tot}} = E_{\infty}^{\text{tot}} + B \exp[-(X - 1)] + C[-(X - 1)^2] \quad (5)$$

proposed by Peterson et al.⁵⁹ and the expression

$$E_X^{\text{tot}} = E_{\infty}^{\text{tot}} + BX^{-3} \quad (6)$$

which is analogous to eq 3, but for the total energy, as used by Dixon et al.³³ for X = (Q,S), henceforth designated as CLASTOT-*n*.

3. RESULTS AND DISCUSSION

The energy profile for the path connecting the two energy regions of the PES for the EGS of the HSO₂ system obtained at the ROCCSD(T)/aV(T+d)Z level is shown in Figure 1. A subscript s will be used to designate skewed conformations of

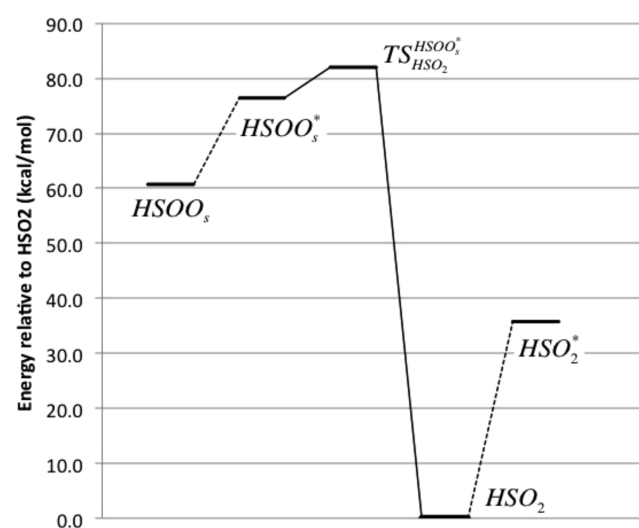


Figure 1. Energy profile showing stationary points of the ground and excited electronic states along the path connecting the two energy regions of the PES for the EGS of the HSO₂ system obtained at the ROCCSD(T)/aV(T+d)Z level, with ZPE correction.

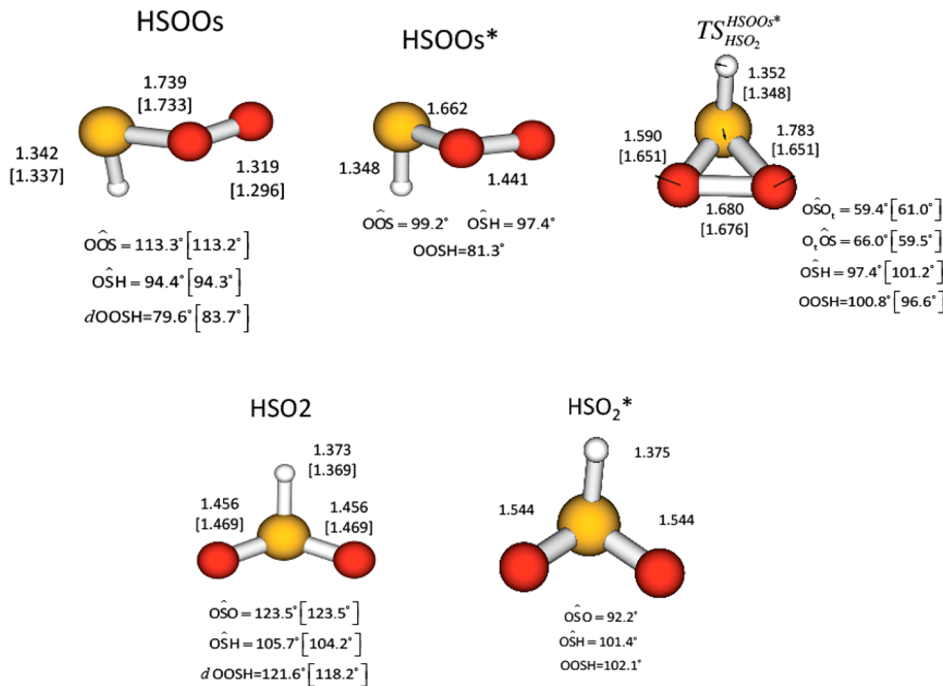


Figure 2. Stationary points connecting the lower and the upper energy regions of the PES for the ground electronic state of the HSO_2 system calculated at the CCSD(T)/aV(T+d)Z level. CASPT2/aV(T+d)Z results are shown in brackets, when applicable. The arrows represent the imaginary normal mode of $\text{TS}_{\text{HSO}_2}^{\text{HOOs}*}$.

any of the species investigated. The solid lines connect HSO_2 , the minimum in the lower energy region of the EGS, and HSOO_s^* , the minimum in the electronic excited state, to the transition state $\text{TS}_{\text{HSO}_2}^{\text{HOOs}*}$. The dashed lines indicate that the connected minima belong to distinct electronic states, as will be further discussed in sections 3.2 and 3.3. The corresponding geometries of the species in Figure 1 are shown in Figure 2, including the arrows representing the displacements associated to the imaginary normal mode of the transition state. When applicable, the geometric parameters from the previous CASPT2/aV(T+d)Z calculations³⁴ are also shown. For structures with nonequivalent oxygen bonds, we distinguish the terminal oxygen atom, or the one involved in the longer S–O bond, with a t subscript (O_t).

The ROCCSD(T) energy profile presents a qualitatively distinct picture from that previously reported.³⁴ The TS_3 and $\text{HSO}_2(\text{b})$ stationary points obtained at the CASPT2 level³⁴ could not be found in the present work. However, we obtained two minima labeled as HSOO_s^* and HSO_2^* , which have not been observed in ref 34 or any other previously reported study of the HSO_2 PES. It is possible that the level of calculations in refs 19, 25, and 34 and/or the region of the PES chosen for investigation in refs 27 and 32 have precluded the determination of the crossing seam observed in the present work. The current results indicate that there is only one transition state along the HSOO_s – HSO_2 minimum energy path as opposed to the two transition states described in ref 34. Although the geometric differences between the $\text{TS}_{\text{HSO}_2}^{\text{HOOs}*}$ transition state and the one denoted $\text{TS}4$ in ref 34 are small, the present structure does not show C_s symmetry, and the S–O bond is almost 0.2 Å shorter than the S– O_t bond.

Relative energies of the optimized stationary points along the HSOO_s – HSO_2 pathway are given in Table 1 together with the corresponding CASPT2 results.³⁴ Inclusion of the ZPE

Table 1. Relative Energies (kcal/mol) of the Stationary Points along the Connection Path

stationary points	CASPT2/ aV(T+d)Z ^a		ROCCSD(T)/ aV(T+d)Z	
	E	ZPE corrected	E	ZPE corrected
HSOO_s – HSOO_s^*			15.2	15.7
HSOO_s^* – $\text{TS}_{\text{HSO}_2}^{\text{HOOs}*}$			7.0	5.6
HSOO_s – $\text{TS}_{\text{HSO}_2}^{\text{HOOs}*}$	12.4	12.1	22.2	21.3
$\text{TS}_{\text{HSO}_2}^{\text{HOOs}*}$ – HSO_2	-93.5	-92.0	-84.7	-82.1
HSO_2 – HSO_2^*			36.5	35.8

^aReference 34.

correction does not change appreciably the reaction profile, the most pronounced effect being the lowering of 2.64 kcal/mol in the $\text{TS}_{\text{HSO}_2}^{\text{HOOs}*}$ – HSO_2 barrier. Frequencies for all the stationary points are given in Table S1 of the Supporting Information, together with data from other selected works for comparison.

3.1. HSOO_s and HSO_2 Isomers. The optimized geometries for the HSOO_s and the HSO_2 species obtained in this work are very similar to those previously reported.³⁴ Also, the differences between the HSOO_s structure obtained in this work and the one obtained by Dixon et al.,³³ at the same level of theory, are negligible, with the bonds and angles differing by less than 0.002 Å and 0.1° (except for the dihedral angle, 4.0° larger than the present value), while the electronic energies differ by only 0.7 mhartree. These small deviations can be attributed to the fact that Dixon et al. have carried out the optimizations with frozen core orbitals and used the spin unrestricted coupled-cluster code subsequent to the ROHF calculations. In the present work, no orbitals were kept frozen, and the coupled-cluster energies were obtained by the spin-restricted method.

The frequencies obtained for the HSOO_s species at the MP2/aV(T+d)Z level by Dixon et al.³³ are reasonably close to our results (differences up to 85 cm^{-1} , at most), and the MP2 zero-point energy is 0.5 kcal/mol higher. Despite the good agreement for individual species, deviations may not be negligible when taking energy differences between stationary points since the errors introduced by taking MP2 frequencies will not necessarily cancel.

Results of vibration frequencies obtained at the CCSD(T) level for the HSO_2 molecule have not been previously reported in the literature, and with the exception of the SH stretch, which is overestimated by $\sim 190 \text{ cm}^{-1}$, our results are within 35 cm^{-1} of the experimental data.²³

3.2. HSOO_s^* and HSOO_s . Inspection of the wave functions associated to the HSOO_s and HSOO_s^* minima reveals that they belong to different doublet electronic states. At the ROCCSD(T) level of calculation, HSOO_s^* is a minimum in the first excited state, vertically 5.9 kcal/mol above the ground state, while HSOO_s is the ground-state minimum, vertically 21.1 kcal/mol below the excited state.

As depicted in Figure 3, while in the HSOO_s wave function, the unpaired electron is basically in an out-of-plane p-type

orbital belonging to the C_s point group. The wave function with an out-of-plane p-type open-shell orbital is a basis for the A'' irreducible representation, while for the in-plane case, the wave function corresponds to an A' state.

Obtaining the states for the planar isomers is straightforward by just selecting the desired symmetry. However, for skewed conformations, the converged state depends on the starting guess orbitals and on the chosen geometry. For a given initial geometry and choice of atomic densities guess, which is the MOLPRO default, the optimization procedure can lead to any of the two states or not converge at all.

At the ROCCSD(T) level of calculation, it is not possible to analytically determine the point of minimum energy in the crossing seam of the two PESs. In order to address this problem at the ROCCSD(T) level, the following strategy was adopted: starting from the optimized geometries, rigid scans were performed, in order to bring each of the geometries in coincidence to the other. The displacement coordinate for these rigid scans were chosen as equally spaced increments corresponding to one-tenth of the difference between each one of the internal coordinates of the HSOO_s and HSOO_s^* optimized geometries.

The energy gap between the two states at the ROCCSD(T) level is shown in Figure 4. The main contribution to the displacement coordinate, in the $\text{HSOO}_s \rightarrow \text{HSOO}_s^*$ direction, is the shortening of the O–S bond and the lengthening of the O–O bond. A crossing between the PESs of the two electronic states is predicted to be energetically less than 1 kcal/mol above the HSOO_s^* minimum, according to this coordinate.

Alternatively, we performed SA-CASSCF(19,11) calculations in order to verify the possibility of crossing. The results of these calculations are shown in Table 2. The point of minimum energy in the crossing seam lies 5.6 kcal/mol above the energy of the HSOO_s^* SA-CASSCF optimized structure and follows the same tendency of O–S bond shortening and O–O bond lengthening relative to the HSOO_s^* SA-CASSCF optimized geometry. The adiabatic electronic energy difference between HSOO_s^* and HSOO_s stationary points at this level of calculation is 12.3 kcal/mol, as opposed to 15.2 kcal/mol at

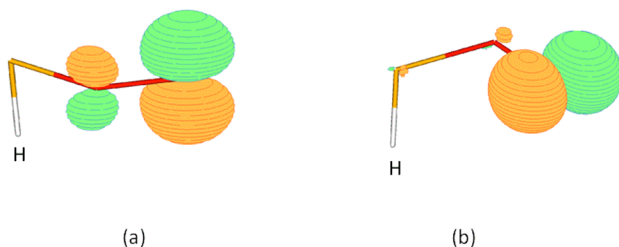


Figure 3. Contour diagrams for HSOO_s (a) and HSOO_s^* (b) open-shell orbitals (contour value = 0.1).

orbital centered on the terminal oxygen atom; for the HSOO_s^* , the unpaired electron is in a similar p-type orbital but oriented in the SOO plane. The distinction becomes clearer when we take the corresponding planar cis or trans structures, which

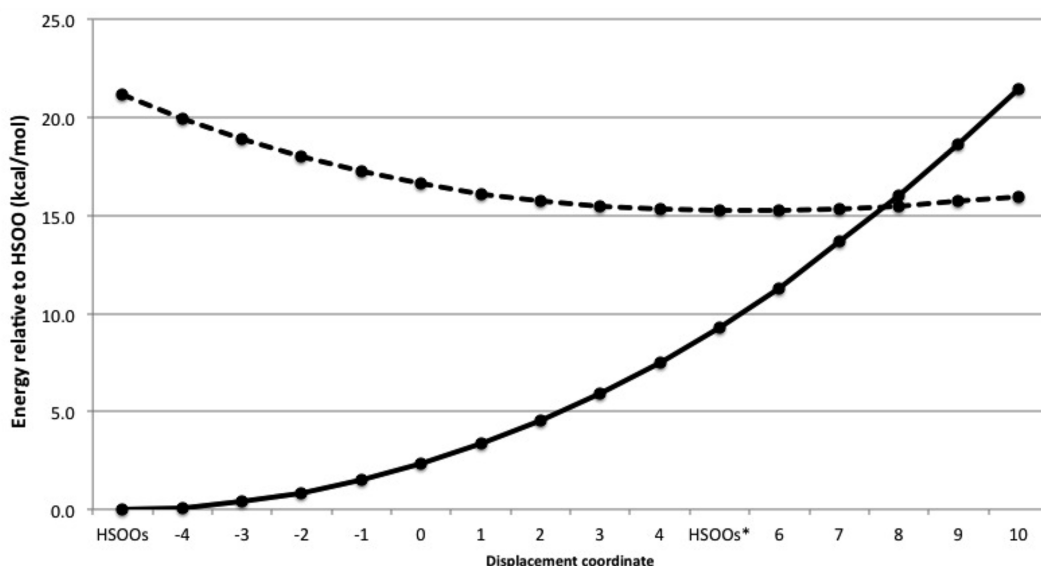


Figure 4. Energy variation of the ground and first excited doublet states along the HSOO_s – HSOO_s^* displacement coordinate, as defined in section 3.2, without ZPE correction.

Table 2. State Average CAS(19,11) Results: Energy of the Ground (E_{GS}) and Excited (E_{ES}) Electronic States (hartree), ΔE (kcal/mol), Interatomic Distances (in Å), and Bond Angles (in degrees)

structure	E_{GS}	E_{ES}	ΔE	$d(O_t-O)$	$d(O-S)$	$d(S-H)$	$\angle(O_tOS)$	$\angle(OSH)$	dihedral
$HSOO_s$	-547.805203	-547.781695	14.8	1.360	1.658	1.328	112.8	96.8	85.8
$HSOO_s^*$	-547.801002	-547.785530	9.7	1.451	1.632	1.331	108.0	98.2	84.2
seam	-547.776645	-547.776645		1.558	1.608	1.336	94.1	100.8	97.8

the ROCCSD(T) level. $HSOO_s^*$ is a minimum vertically 9.7 kcal/mol above the ground state, while $HSOO_s$ is vertically 14.8 kcal/mol below the excited state.

The qualitative agreement between the ROCCSD(T) and SA-CASSCF(19,11) results allow us to conclude that the species $HSOO_s$ and $HSOO_s^*$ are minima in different electronic states, which are connected by a crossing seam. The structure of minimum energy in the seam should have a longer O–O bond and a shorter O–S bond than those of the $HSOO_s^*$ species, and its energy should be at most a few kcal/mol higher than that of the $HSOO_s^*$.

3.3. HSO_2^* and HSO_2 . The optimized structures of the HSO_2 and HSO_2^* species also belong to different doublet electronic states as can be inferred from the inspection of the respective wave functions. The open shell orbitals for both structures are shown in Figure 5. The point group for both

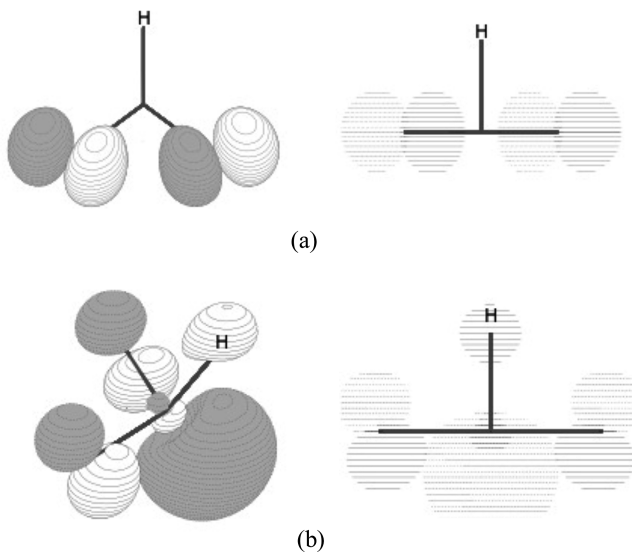


Figure 5. Three- and two-dimensional side-view contour diagrams for HSO_2^* (a) and HSO_2 (b) open shell orbitals (contour = 0.1).

structures is C_s , but now, the symmetry plane is perpendicular to the OSO plane. The HSO_2 structure corresponds to a minimum in the PES for a state of symmetry A' and its open-shell orbital is mainly composed of a combination of two equivalent p-type oxygen orbitals (perpendicular to the OSO plane) and a lobe over the sulfur atom, resembling a lone pair orbital. The HSO_2^* structure corresponds to a minimum in the PES of a state with A'' symmetry and its open shell orbital may be regarded as a combination of two p-type oxygen atoms within the OSO plane.

The energy gap between the two states at the ROCCSD(T) level is shown in Figure 6 along a HSO_2 – HSO_2^* displacement coordinate analogous to the coordinate defined in the previous section. HSO_2 is a minimum in the ground state vertically 76.7 kcal/mol below the first excited state. HSO_2^* is a minimum for the excited state, vertically 2.5 kcal/mol below the ground-state.

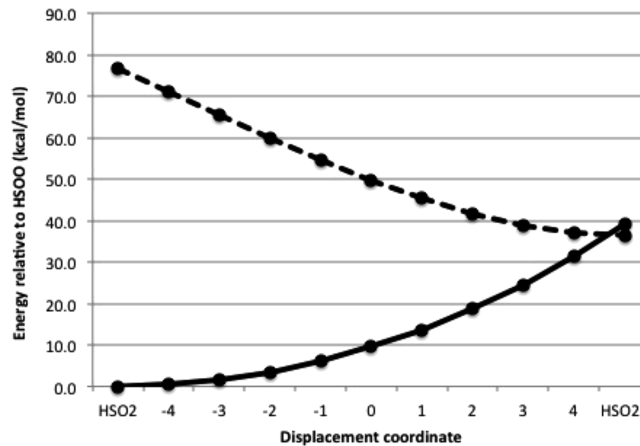


Figure 6. Electronic energy variation of the ground and first excited doublet states along the HSO_2 – HSO_2^* displacement coordinate, as defined in section 3.3.

From Figure 6, it can be estimated that the crossing between A' and the A'' SEPs occurs at 2.9 kcal/mol above the HSO_2^* minimum.

The point of minimum energy in the crossing seam was again determined at the CASSCF(19,11) level, and the HSO_2 and HSO_2^* structures were reoptimized at this level of calculation using symmetry adapted orbitals ($5a' + 2a''$ and $7a' + 4a''$ orbitals for the closed and active spaces, respectively). From the results of the CASSCF calculations gathered in Table 3, it can be noticed that the structure corresponding to the crossing point in the seam is not symmetric and lies only 1.3 kcal/mol below the HSO_2^* energy. The qualitative agreement between the CASSCF and ROCCSD(T) results indicate that HSO_2 and HSO_2^* are minima for different electronic states and that they can be connected by a crossing seam.

3.4. $HSOO_s^* \rightarrow TS_{HSO_2}^{HSOO_s^*}$ Path. The IRC plot in Figure 7 shows a smooth connection between $TS_{HSO_2}^{HSOO_s^*}$ and $HSOO_s^*$ structures. It could be expected, though, that the transition state would connect to the $HSOO_s$ structure since the crossing seam is predicted to be energetically very close to $TS_{HSO_2}^{HSOO_s^*}$. However, inspection of open-shell orbitals for both stationary points and selected IRC points (Figure 8) clarifies how the SCF procedure of the ROHF step manages to keep the valence orbital lying in the SOO plane and therefore remaining in the same electronic state. Nevertheless, depending on the wave function chosen as the reference for the CCSD(T) step, it is possible that the open-shell orbital will rotate to the out-of-plane orientation of the ground electronic state in which case the IRC would lead to the $HSOO_s$ structure. Hence, although $TS_{HSO_2}^{HSOO_s^*}$ and $HSOO_s^*$ structures are connected by the IRC, it would be more appropriate to consider the energy barrier for the reaction relative to the ground-state $HSOO_s$ energy, which is 21.3 kcal/mol at the ROCCSD(T) level.

Table 3. CAS(19,11) Results with Symmetry Adapted Orbitals: Energies (hartree), ΔE (kcal/mol), Interatomic Distances (in Å), and Bond Angles (in degrees)

structure	E (A' state)	E (A'' state)	ΔE	$d(S-O_t)$	$d(S-O)$	$d(S-H)$	$\angle(OSO_t)$	$\angle(OSH)$	dihedral
HSO_2^a	-547.864933	-547.743858	76.0	1.428	1.428	1.342	126.0	106.0	124.2
HSO_2^{*b}	-547.805505	-547.811801	-4.0	1.522	1.522	1.346	98.3	100.7	102.7
seam	-547.813870	-547.813870		1.714	1.424	1.368	91.8	113.7	113.7

^aUsing the optimized structure with A' symmetry. ^bUsing the optimized structure with A'' symmetry.

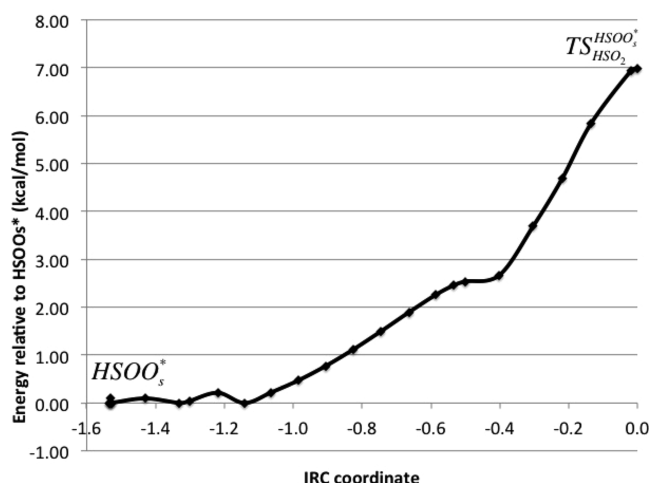


Figure 7. IRC path connecting $TS_{HSO_2}^{HSOO_s^*}$ and $HSOO_s^*$ stationary points.

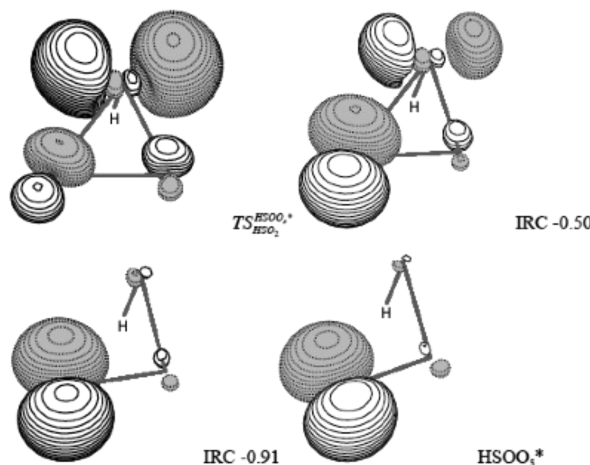


Figure 8. Contour diagrams of open-shell orbitals for selected points along the IRC path connecting $TS_{HSO_2}^{HSOO_s^*}$ and $HSOO_s^*$ stationary points (contour value = 0.1).

3.5. $TS_{HSO_2}^{HSOO_s^*}$ – HSO_2 Path. The connection between $TS_{HSO_2}^{HSOO_s^*}$ and HSO_2 could not be achieved in a single continuous run, as indicated in Figure 9. Starting from the transition state structure, the SCF procedure would not converge for the second IRC point, regardless of the convergence parameters chosen. Nonetheless, convergence is achieved when atomic densities are used as the starting orbital guess, and the IRC could be restarted from that point. The open-shell orbital changes significantly, adopting a O–O σ^* character (Figure 10), and the bond dissociation seems to proceed correctly.

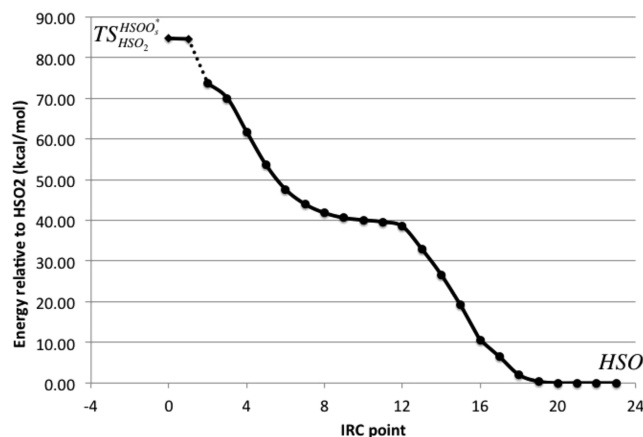


Figure 9. IRC path connecting $TS_{HSO_2}^{HSOO_s^*}$ and HSO_2 stationary points.

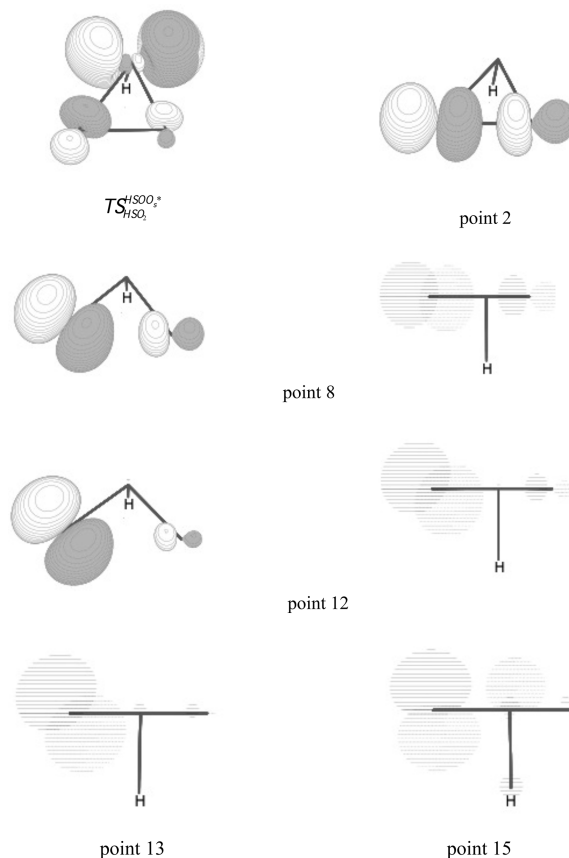


Figure 10. Contour diagrams of open-shell orbitals for selected points along the IRC path connecting $TS_{HSO_2}^{HSOO_s^*}$ and HSO_2 stationary points (contour value = 0.1).

As one inspects the open-shell orbital of the structure corresponding to the IRC point 2 (the restarting point), the

resemblance with the corresponding orbital of the HSO_2^* structure becomes evident, suggesting that the IRC should connect these structures. However, contrary to what was observed in the $\text{TS}_{\text{HSO}_2} \rightarrow \text{HSOO}_s^*$ path, snapshots of the open-shell orbital along the IRC (Figure 10) clearly show that, during the SCF procedure, the orbital smoothly rotates from the in-plane orientation to an out-of-plane orientation (with respect to the OSO plane), keeping the structures in the ground electronic state PES and heading to the HSO_2 minimum.

At point 16, SCF failed to converge again, but this time, convergence could be achieved by just increasing the maximum number of iterations and disabling the DIIS accelerating method. Thus, this apparent failure to converge at point 16 can be attributed to the large change in the open-shell orbital, from point 15 to 16 (Figure 9), precluding the SCF procedure to converge with the default parameters.

3.6. Additional Stationary Points. Besides the stationary points directly involved in the connecting path under investigation, other structures are important to characterize the profile of this region of the PES, although with no major implications to the reaction path. These other structures are rotamers of HSOO_s and HSOO_s^* , i.e., very similar structures but with distinct dihedral angles, and the respective transition states connecting the HSOO_s^* enantiomers. These structures are collected in Figure 11, except for the ones already presented

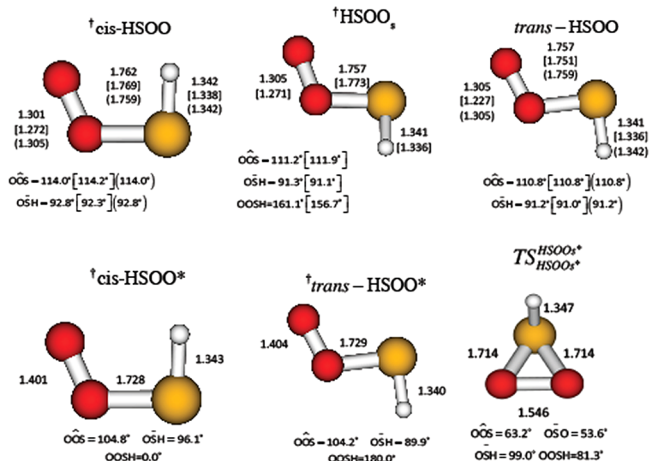


Figure 11. Additional stationary points of the upper energy region of the HSO_2 PES calculated at the CCSD(T)/aV(T+d)Z level. Corresponding CASPT2³⁴ and CCSD(T)³³ results are, respectively, shown in brackets and in parentheses.

in Figure 2, and their vibration frequencies are shown in Table S1 of the Supporting Information. For the rotamers, the transition state structures will be distinguished from the other stationary points by the \dagger superscript.

The optimized geometries for HSOO_s minimum and its $\dagger\text{cis-HSOO}$ and trans-HSOO rotamers are practically indistinguishable from the ones obtained by Dixon et al.³³ However, Dixon has assigned the trans-HSOO as a transition state, while the present results indicate that it should be a minimum in which case an additional transition state must exist, in accordance with CASPT2 results.³⁴ The IRC plotted as a function of the dihedral angle is shown in Figure 12. As noticed in the aforementioned articles, these structures are energetically very close, considering that the largest barrier is only 1.0 kcal/mol

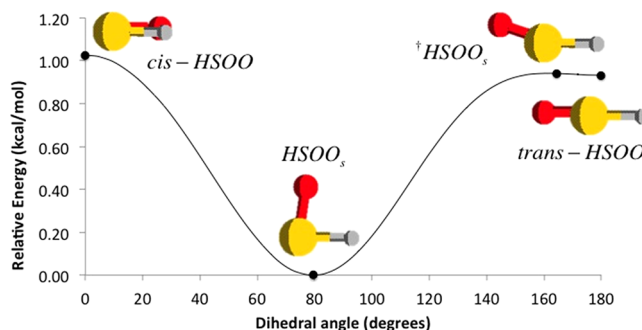


Figure 12. IRC connecting the HSOO rotamers as a function of the dihedral angle.

using the aV(T+d) basis set. The energy profile for HSOO_s^* , though, is much more sensitive to the S–H rotation since, from the data in Table S2, the barrier to $\dagger\text{cis-HSOO}^*$ is 9.1 kcal/mol and 9.6 kcal/mol to $\dagger\text{trans-HSOO}^*$, including ZPE.

Additionally, there is a $\text{TS}_{\text{HSOO}_s^*}$ structure that connects the two HSOO_s^* enantiomers, exhibiting C_s symmetry, and the barrier for this isomerization is 5.1 kcal/mol.

3.7. CBS Extrapolations. Absolute extrapolated energies are compiled in Table S2 of the Supporting Information. As discussed in section 2, the CBS studies were carried out with the aV(X+d)Z basis sets, with X = 3–5. However, since we can afford calculations with the aV(6+d)Z basis at the HF level, in order to assess the reliability of HF-2 and HF-3 schemes, Hartree–Fock energies were also obtained for HSO_2 and cis-HSOO structures with that basis set and then compared to the corresponding predicted extrapolated energies. While HF-3 extrapolated energies were indeed lower than the calculated one with the aV(6+d) basis set, the HF-2 extrapolated energies were 0.35 and 0.06 mhartree higher than the Hartree–Fock energies for HSO_2 and cis-HSOO , respectively. Therefore, we shall compare PET-3 and CLASTOT-n directly with the total energies obtained by adding HF-3 extrapolated ROHF energies to CLAS-n and USTE-n correlation energies.

Let us first examine the general behavior of different CBS correction methods by looking at the relative energies among the optimized structures. A comparison of the energies obtained with the aV(T+d) basis set and the distinct CBS methods, for the HSOO_s and HSOO_s^* species relative to their respective rotamers (Table 4), shows that the CBS corrections are practically the same and almost negligible ($|\Delta E| \leq 0.06$ kcal/mol), except for some CLASTOT-3 results. The energy barriers between HSOO_s and HSOO_s^* and $\text{TS}_{\text{HSO}_2}^*$ are lowered by 1.60–1.65 kcal/mol with CBS corrections, while the reverse barrier $\text{HSO}_2 - \text{TS}_{\text{HSO}_2}^*$ increases roughly by 4.20–4.30 kcal/mol. The HSOO_s^* isomerization barrier lowers by 1.75 kcal/mol with basis set extrapolation. Additionally, it is noticeable the agreement between the CLAS-2 and USTE-2 predicted corrections and also that corrections obtained with the CLAS-3 and USTE-3 methods are exactly the same, in kcal/mol, within two decimal places.

It is not straightforward to decide which CBS extrapolation scheme is the most accurate, especially when reliable experimental data or calculations with more complete basis sets are not available. However, from the results shown on Tables 4 and S2 (Supporting Information), it seems that,

Table 4. Comparison between the Relative Energy (ΔE) of Several Pairs of Stationary Points Computed with the aug-cc-pV(T+d) and Different Complete Basis Set (CBS) Extrapolations Schemes (See Section 2)

ΔE (kcal/mol)	HF-3/CLAS-2	HF-3/USTE-2	CLASTOT-2	HF-3/CLAS-3	HF-3/USTE-3	CLASTOT-3	PET-3
TS _{HSO₂} ^{HOO*} –HSOO _s *	-1.64	-1.64	-1.71	-1.66	-1.66	-1.71	-1.55
TS _{HSO₂} ^{HOO*} –HSOO _s	-1.62	-1.61	-1.68	-1.62	-1.63	-1.56	-1.49
TS _{HSO₂} ^{HOO*} –HSO ₂	4.29	4.27	4.52	4.19	4.19	4.35	4.04
HSO ₂ –HSO ₂ *	2.30	2.29	2.44	2.29	2.29	2.32	2.18
TS _{HSO₂} ^{HOO*} –HSOO _s *	-1.74	-1.73	-1.79	-1.76	-1.77	-1.78	-1.62
HSOO _s *–HSOO _s	0.02	0.02	0.03	0.04	0.03	0.15	0.05
trans-HSOO*–HSOO _s *	0.05	0.05	0.04	0.03	0.03	-0.01	0.03
[†] cis-HSOO*–HSOO _s *	-0.02	-0.02	-0.02	-0.03	-0.03	-0.07	-0.03
[†] cis-HSOO–HSOO _s	-0.05	-0.05	-0.06	-0.06	-0.06	-0.08	-0.06
[†] HSOO _s –HSOO _s	-0.06	-0.06	-0.06	-0.06	-0.06	-0.08	-0.06
[†] HSOO _s –trans-HSOO	0.01	0.01	0.01	0.02	0.02	0.02	0.01

overall, the PET-3 CBS scheme gives the most reliable extrapolated results for the species investigated.

4. CONCLUSIONS

Ab initio calculations at the ROCCSD(T)/aug-cc-pV(X+d)Z level with X = T,Q,S have been reported for the stationary states along the path connecting the high and low energy regions of the HSO₂ potential energy surface. The present calculations confirm the proposition made by Garrido et al.³⁴ about the connection of the HSOOs structure belonging to the high energy part of the PES, with the HSO₂ minima, located in the low energy region. However, the calculations at the ROCCSD(T) level show that there is only one transition state in the path, in contrast to previous CASPT2 predictions.³⁴ It has been found that the structures relevant to this connection may belong to different electronic states and that the presence of crossing seams have been confirmed by SA-CASSCF calculations. Several methods for CBS energy extrapolation were evaluated with the conclusion that the 3-parameter scheme proposed by Peterson et al.⁵⁹ (PET-3) gives the most reliable energies for the studied system. Finally, the possibility of the direct reaction SH + O₂ → H + SO₂ is indirectly confirmed by the reaction HSOO_s → HSO₂. Nevertheless, the inclusion of the calculated stationary states in the context of the global HSO₂ PES is necessary in order to assess the implications of the present results to chemical parameters such as rate constants and reaction cross-sections.

■ ASSOCIATED CONTENT

Supporting Information

Vibration frequencies for calculated points of the HSO₂ PES; ROCCSD(T)/aug-cc-pV(X+d)Z energies with X = T,Q,S in atomic units; CBS extrapolation energies in atomic units. This material is available free of charge via the Internet at <http://pubs.acs.org>.

■ AUTHOR INFORMATION

Corresponding Author

*Phone: +55-21-2562-7563. Fax: +55-21-2562-7265. E-mail: chaer01@gmail.com.

Notes

The authors declare no competing financial interest.

■ ACKNOWLEDGMENTS

This work has been partially supported by CNPq and FAPERJ. J.D.G., in particular, thanks FAPERJ for a visiting professor scholarship and Diana Rodríguez Linares for discussions.

■ REFERENCES

- Wayne, R. P. *Chemistry of Atmospheres*; Oxford University Press: New York, 2002.
- Finlayson-Pitts, B. J.; Pitts, J. N., Jr. *Chemistry of the Upper and Lower Atmosphere*; Academic Press: San Diego, CA, 2000.
- Warneck, P. *Chemistry of the Natural Atmospheres*; Academic Press: New York, 1988.
- Arutyunov, V. A.; Vedeneev, V. I.; Ushakov, V. A.; Shumova, V. V. *Kinet. Katal.* **1990**, *31*, 6.
- Tsuchiya, K.; Kamiya, K.; Matsui, H. *Int. J. Chem. Kinet.* **1997**, *29*, 57–66.
- Cerru, F. G.; Kronenburg, A.; Lindstedt, R. P. *Proc. Combust. Inst.* **2005**, *30*, 1227–1235.
- Glarborg, P. *Proc. Combust. Inst.* **2007**, *31*, 77–98.
- Boyd, R. J.; Gupta, A.; Langler, R. F.; Lownie, S. P.; Pincock, J. A. *Can. J. Chem.* **1980**, *58*, 331–338.
- Hinchliffe, A. J. *Mol. Struct.* **1981**, *71*, 349–352.
- Binns, D.; Marshall, P. *J. Chem. Phys.* **1991**, *95*, 4940–4947.
- Laakso, D.; Marshall, P. *J. Chem. Phys.* **1992**, *96*, 2471–2474.
- Laakso, D.; Smith, C. E.; Goumri, A.; Rocha, J.-D. R.; Marshall, P. *Chem. Phys. Lett.* **1994**, *227*, 377–383.
- Morris, V. R.; Jackson, W. M. *Chem. Phys. Lett.* **1994**, *223*, 445–451.
- Goumri, A.; Rocha, J.-D. R.; Marshall, P. *J. Phys. Chem.* **1995**, *99*, 10834–10836.
- Frank, A. J.; Sadílek, M.; Ferrier, J. G.; Tureček, F. *J. Am. Chem. Soc.* **1996**, *118*, 11321–11322.
- Qi, J.-X.; Deng, W.-Q.; Han, K.-L.; He, G.-Z. *J. Chem. Soc. Faraday Trans.* **1997**, *93*, 25–28.
- Frank, A. J.; Sadílek, M.; Ferrier, J. G.; Tureček, F. *J. Am. Chem. Soc.* **1997**, *119*, 12343–12353.
- Drozdova, Y.; Steudel, R.; Hertwig, R. H.; Koch, W.; Steiger, T. *J. Phys. Chem. A* **1998**, *102*, 990–996.
- Goumri, A.; Rocha, J.-D. R.; Laakso, D.; Smith, C. E.; Marshall, P. *J. Phys. Chem. A* **1999**, *103*, 11328–11335.
- Isoniemi, E.; Khriachtchev, L.; Lundell, J.; Räsänen, M. *J. Mol. Struct.* **2001**, *563–564*, 261–265.
- Denis, P. A.; Ventura, O. N. *Chem. Phys. Lett.* **2001**, *344*, 221–228.
- McKee, M. L.; Wine, P. H. *J. Am. Chem. Soc.* **2001**, *123*, 2344–2353.
- Isoniemi, E.; Khriachtchev, L.; Lundell, J.; Räsänen, M. *Phys. Chem. Chem. Phys.* **2002**, *4*, 1549–1554.
- Wang, L.; Zhang, J. *Mol. Struct.* **2002**, *581*, 129–138.

- (25) Resende, S. M.; Ornellas, F. R. *Phys. Chem. Chem. Phys.* **2003**, *5*, 4617–4621.
- (26) Wang, B.; Hou, H. *Chem. Phys. Lett.* **2005**, *410*, 235–241.
- (27) Ballester, M. Y.; Varandas, A. J. C. *Phys. Chem. Chem. Phys.* **2005**, *7*, 2305–2317.
- (28) Napolion, B.; Watts, J. D. *Chem. Phys. Lett.* **2006**, *421*, 562–565.
- (29) Wierzejewska, M.; Olbert-Majkut, A. *J. Phys. Chem. A* **2007**, *111*, 2790–2796.
- (30) Midey, A. J.; Viggiano, A. A. *J. Phys. Chem. A* **2007**, *111*, 1852–1859.
- (31) Wheeler, S. E.; Schaefer, H. F., III. *J. Phys. Chem. A* **2009**, *113*, 6779–6788.
- (32) Zhou, C.; Sendt, K.; Haynes, B. S. *J. Phys. Chem. A* **2009**, *113*, 2975–2981.
- (33) Grant, D. J.; Dixon, D. A.; Francisco, J. S.; Feller, D.; Peterson, K. A. *J. Phys. Chem. A* **2009**, *113*, 11343–11353.
- (34) Garrido, J. D.; Ballester, M. Y.; Orozco-González, Y.; Canuto, S. *J. Phys. Chem. A* **2011**, *115*, 1453–1461.
- (35) Knowles, P. J.; Hampel, C.; Werner, H.-J. *J. Chem. Phys.* **1993**, *99*, 5219–5227.
- (36) Knowles, P. J.; Hampel, C.; Werner, H.-J. *J. Chem. Phys.* **2000**, *112*, 3106–3107.
- (37) Watts, J. D.; Gauss, J.; Bartlett, R. J. *J. Chem. Phys.* **1993**, *98*, 8718–8733.
- (38) Korona, T.; Jeziorsky, B. *J. Chem. Phys.* **2006**, *125*, 184109–184121.
- (39) Jeziorsky, B.; Moszynski, R. *Int. J. Quantum Chem.* **1993**, *48*, 161–183.
- (40) Dunning, T. H., Jr. *J. Chem. Phys.* **1989**, *90*, 1007–1023.
- (41) Kendall, R. A.; Dunning, T. H., Jr.; Harrison, R. J. *J. Chem. Phys.* **1992**, *96*, 6796–6806.
- (42) Martin, J. M. L. *J. Chem. Phys.* **1998**, *108*, 2791–2800.
- (43) Martin, J. M. L.; Uzan, O. *Chem. Phys. Lett.* **1998**, *282*, 16–24.
- (44) Bauschlicher, C. W., Jr.; Ricca, A. *J. Phys. Chem.* **1998**, *102*, 8044–8050.
- (45) Bauschlicher, C. W., Jr.; Partridge, H. *Chem. Phys. Lett.* **1995**, *240*, 533–540.
- (46) Dunning, T. H., Jr.; Peterson, K. A.; Wilson, A. K. *J. Chem. Phys.* **2001**, *114*, 9244–9253.
- (47) Peterson, K. A.; Woon, D. E.; Dunning, T. H., Jr. *J. Chem. Phys.* **1993**, *100*, 7410–7415.
- (48) Fukui, K. *J. Phys. Chem.* **1970**, *74*, 4161–4163.
- (49) Werner, H. J.; Knowles, P. J.; Lindh, R.; Manby, F. R.; Schütz, M.; Celani, P.; Korona, T.; Rauhut, G.; Amos, R. D.; Bernhardsson, A.; et al. *MOLPRO*, version 2009.1, a package of ab initio programs; Universität Stuttgart: Stuttgart, Germany; see <http://www.molpro.net>.
- (50) Diffender, R. N.; Yarkony, D. R. *J. Phys. Chem.* **1982**, *86*, 5098.
- (51) Lischka, H.; Shepard, R.; Shavitt, I.; Pitzer, R. M.; Dallos, M.; Müller, T.; Szalay, P. G.; Brown, F. B.; Ahlrichs, R.; Böhm, H. J.; et al. *COLUMBUS*, release 5.9.2, an ab initio electronic structure program; University of Vienna: Vienna, Austria, 2008.
- (52) Banerjee, A.; Adams, N.; Simons, J. *J. Phys. Chem.* **1985**, *89*, 52–57.
- (53) Sendt, K.; Haynes, B. S. *Proc. Combust. Inst.* **2007**, *31*, 257–265.
- (54) Feller, D. *J. Chem. Phys.* **1993**, *98*, 7059–7071.
- (55) Jensen, F. *Theor. Chem. Acc.* **2005**, *113*, 8880.
- (56) Karton, A.; Martin, J. M. L. *Theor. Chem. Acc.* **2006**, *115*, 330–333.
- (57) Helgaker, T.; Klopper, W.; Koch, H.; Noga, J. *J. Chem. Phys.* **1997**, *106*, 9639–9646.
- (58) Varandas, A. J. *J. Chem. Phys.* **2007**, *126*, 244105.
- (59) Peterson, K. A.; Woon, D. E.; Dunning, T. H., Jr. *J. Chem. Phys.* **1994**, *100*, 7410–7415.